Preprint Title	Synthesis and Properties of Tetrathiafulvalenes Bearing 6-Aryl-1,4-dithiafulvenes
Authors	Aya Yoshimura, Hitoshi Kimura, Kohei Kagawa, Mayuka Yoshioka, Toshiki Itou, Dhananjayan Vasu, Takashi Shirahata, Hideki Yorimitsu and Yohji Misaki
Publication Date	12 Feb 2020
Article Type	Full Research Paper
Supporting Information File 1	DT-Aryl-TTF_SI.pdf; 8.4 MB
ORCID® iDs	Takashi Shirahata - https://orcid.org/0000-0003-0899-3767; Hideki Yorimitsu - https://orcid.org/0000-0002-0153-1888; Yohji Misaki - https://orcid.org/0000-0002-9079-8487

Synthesis and Properties of Tetrathiafulvalenes Bearing 6-Aryl-1,4-dithiafulvenes

Aya Yoshimura[1,2], Hitoshi Kimura[1], Kohei Kagawa[1], Mayuka Yoshioka[1], Toshiki Itou[1], Dhananjayan Vasu[3], Takashi Shirahata[1,2], Hideki Yorimitsu[3], Yohji Misaki*[1,2]

Address: [1]Department of Materials Science and Biotechnology, Graduate School of Science and Engineering, Ehime University, 3 Bunkyo-cho, Matsuyama, Ehime 790-8577, Japan, [2]Research Unit for Power Generation and Storage Materials, and Research Unit for Development of Organic Superconductors, Ehime University, Matsuyama, Ehime 790-8577, Japan, and [3]Department of Chemistry, Graduate School of Science, Kyoto University, Sakyo-ku, Kyoto 606-8502, Japan

Email: Yohji Misaki – misaki.yohji.mx@ehime-u.ac.jp

* Corresponding author

Abstract

Novel multistage redox TTFs bearing 6-aryl-1,4-dithiafulvene moieties were synthesized by using the palladium-catalyzed direct C-H arylation. In the presence of a catalytic amount of $Pd(OAc)_2$, P^tBu_3•HBF_4, and excess amount of Cs_2CO_3, the C-H arylation of TTF with several aryl bromides bearing 1,3-dithiol-2-ylidenes took place efficiently to produce the corresponding π-conjugation molecules. We also succeeded in estimation of the oxidation potentials and number of electrons involved in each oxidation step of the obtained compounds by the digital simulations.

Keywords

tetrathiafulvalene; extended π-conjugation; cross-conjugated systems; electrochemical properties; digital simulation analysis

Introduction

Tetrathiafulvalene (TTF) with extended π-conjugation have attracted attention as possible components for functional materials such as molecular conductors, field-effect transistor (FET), and positive electrode materials for rechargeable batteries, because the TTF moiety has strong electron-donating properties attributed to the formation of stable aromatic 1,3-dithiol-2-ylidenes (1,3-dithiole rings) by one- and two-electron oxidation [1-16]. Considerable efforts have been devoted to the development of peripherally benzene- or thiophene-substituted TTFs. As for peripherally benzene-functionalized TTFs, some synthetic approaches, crystal and electron structures, electrochemical and optical properties, and the nature of ion-radical complexes with DDQ or iodine were reported [17-24]. Peripherally thiophene-functionalized TTFs as potential precursors to conducting polymers and organic metals were also prepared and characterized [25-29]. To design more tempting molecules, 1,3-dithiole rings on aromatic rings appears very appealing since they allow to produce novel multistage redox systems. However, such molecules could not be synthesized by conventional approaches. In 2011, a breakthrough synthesis of arylated TTF derivatives by using palladium-catalyzed direct C-H arylation was reported and their structural and electrochemical properties were clarified [30]. This motivated us to synthesize the novel multistage redox TTFs bearing 1,3-dithiole rings on aromatic rings **1–3** (Chart 1).

In addition, we have focused on cross-conjugated systems with 1,3-dithiole rings, which are of interest as novel multistage redox systems as well as donor component for organic conductors [1,31-41]. The palladium-catalyzed C-H arylation might offer new cross-conjugated molecules bearing conjugated moieties at the peripheral part of TTF, such as **4** (Chart 1), and its electrochemical property should be brought to light. Herein, we report the synthesis and electrochemical properties of **1–4**.

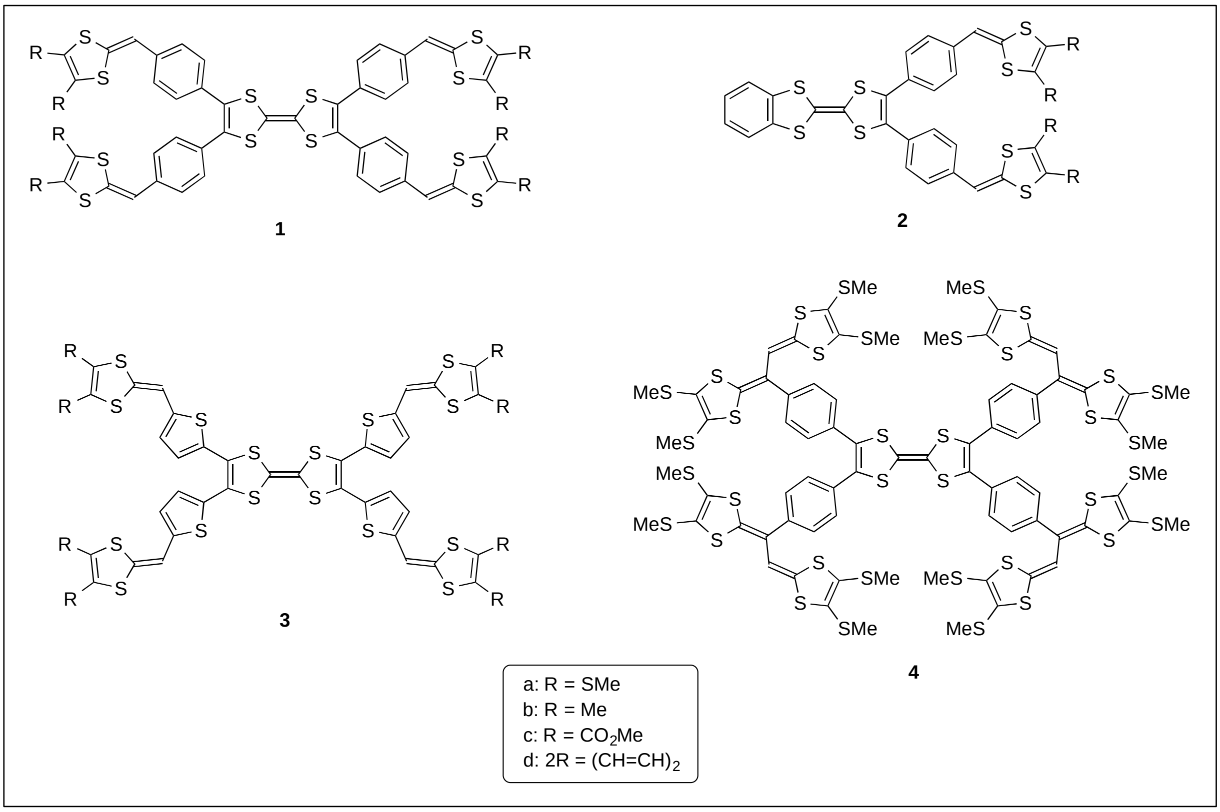

Chart 1: Target compounds.

Results and Discussion

We tried to synthesize compounds **1** and **2** in one step from pristine TTF and **5**, respectively, through the palladium-catalyzed C-H arylation (Table 1). Aryl bromides **6a,b** were allowed to react with TTF under the condition A, the products **1a,b** were produced in 46 and 48% yields, respectively (entries 1 and 2). In contrast, **1c,d** were obtained in low yields as a mixture of hardly separable mono-, di-, tri-, and tetraarylated TTFs under the conditions both A and B (entries 3 and 4). The palladium-catalyzed C-H arylation of **5** with **6a,b** also proceeded to give **2a,b** in 75 and 86% yields, respectively (entries 5 and 6). On the other hand, it was difficult to produce **3** in the same manner because 2-bromothiophenes **7** bearing a 1,3-dithiole ring at the 5-position were unstable, for example, **7c** was decomposed at around 67 °C (Scheme 1a). Therefore, we could achieve the synthesis of **3a** by the Pd-catalyzed thienylation of TTF using acetal-protected **8** and the following deprotection using PTSA•H_2O and the $P(OEt)_3$-mediated cross coupling with **11** (Scheme 1b). Cross-conjugated molecule **4** was prepared in two procedures, one is the palladium-catalyzed C-H arylation of TTF with bromide **12** (Scheme 2a) and the other is the Vilsmeier-Haack reaction of **1a** and the following triethyl phosphite-mediated cross coupling with **11** (Scheme 2b).

Table 1: Synthesis of compounds **1** and **2**.

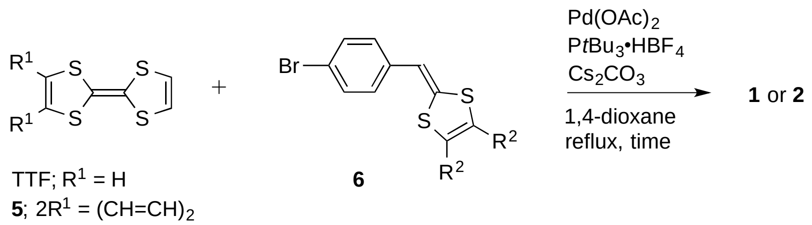

condition A; 30 mol% $Pd(OAc)_2$, 90 mol% P*t*Bu_3•HBF_4 6 equiv Cs_2CO_3, 36 h
B; 60 mol% $Pd(OAc)_2$, 180 mol% P*t*Bu_3•HBF_4 12 equiv Cs_2CO_3, 108 h

entry	TTF or **5**	**6** (equivalent)	condition	yields of **1** or **2** (%)
1	TTF	**6a** (5)	A	**1a**; 46
2	TTF	**6b** (5)	A	**1b**; 48
3	TTF	**6c** (5)	A or B	**1c**; 0 (mixture)
4	TTF	**6d** (5)	A or B	**1d**; 0 (mixture)
5	**5**	**6a** (2.5)	A[a)]	**2a**; 75

6	**5**	**6b** (2.5)	A[a)]	**2b**; 86

[a] 24 h.

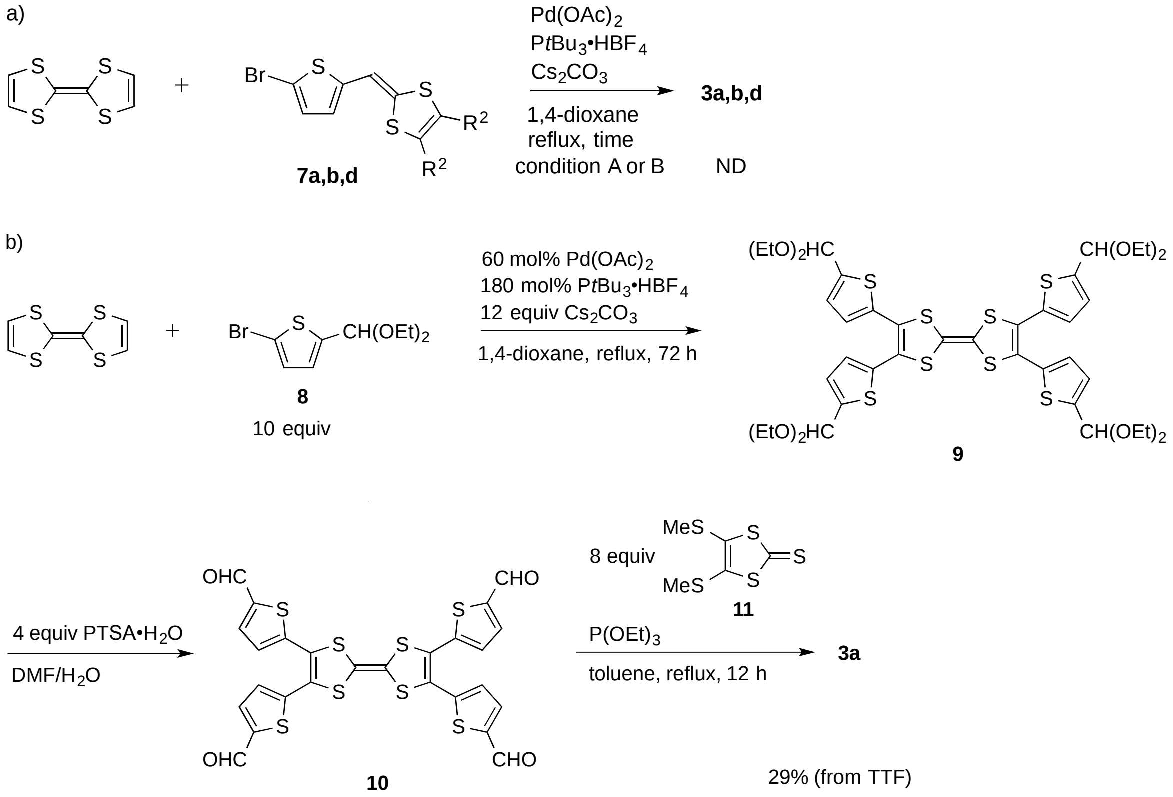

Scheme 1: Synthesis of compound **3**.

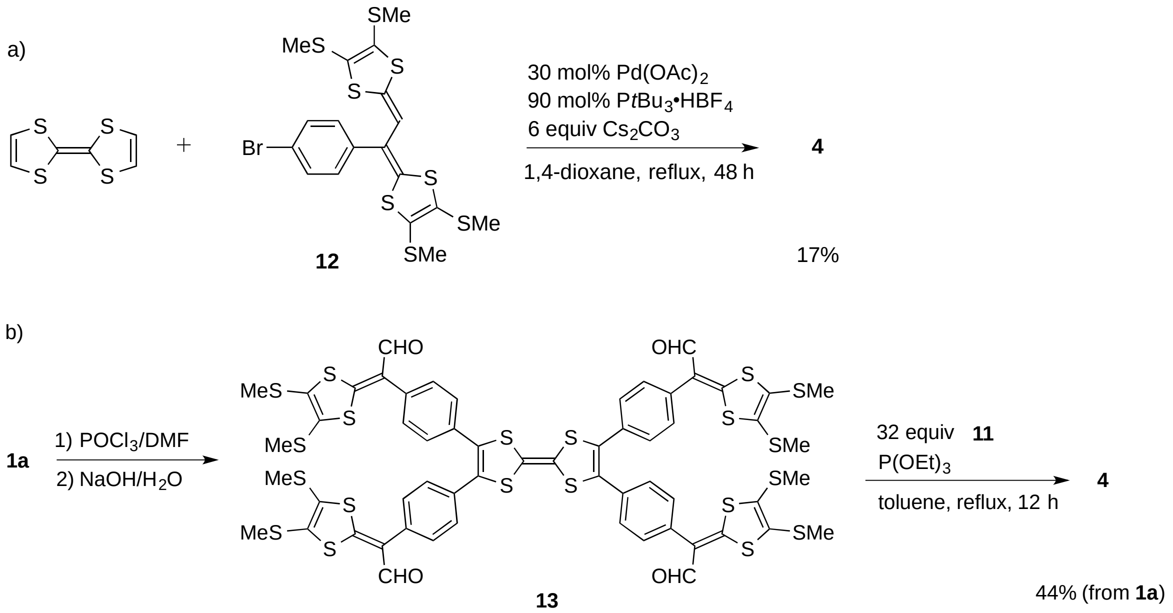

Scheme 2: Synthesis of compound **4**.

The molecular orbital calculation of **1a**, **3a** and **4** has been carried out by using B3LYP/6-31G(d) method [42]. Figure 1 shows an optimized geometry of **1a**, and 1,3-dithiole rings are labeled with A–E and A'–E'. This molecule adopts a nonplanar structure. The angles between two 1,3-dithiole rings in the center (A–A') is 155.5º. The dihedral angles between A and B, A and B', A' and C, and A' and C' were 137.9º, 48.5º, 48.6º, and 136.6º, respectively. The HOMO, HOMO–1, and LUMO of **1a** are shown in Figure 2. The HOMO of **1a** is mainly located on the TTF moiety, whereas the HOMO–1 is located on the benzene and outer 1,3-dithiole rings at the peripheral part of TTF. The LUMO of **1a** spreads over the whole molecule except the outer 1,3-dithiole rings. The orbital energy of HOMO of **1a** (–4.33 eV) is higher than that of TTF (–6.38 eV). If the oxidation relates to the orbital energy, the first oxidation of **1a** might occur at lower potential than TTF [43].

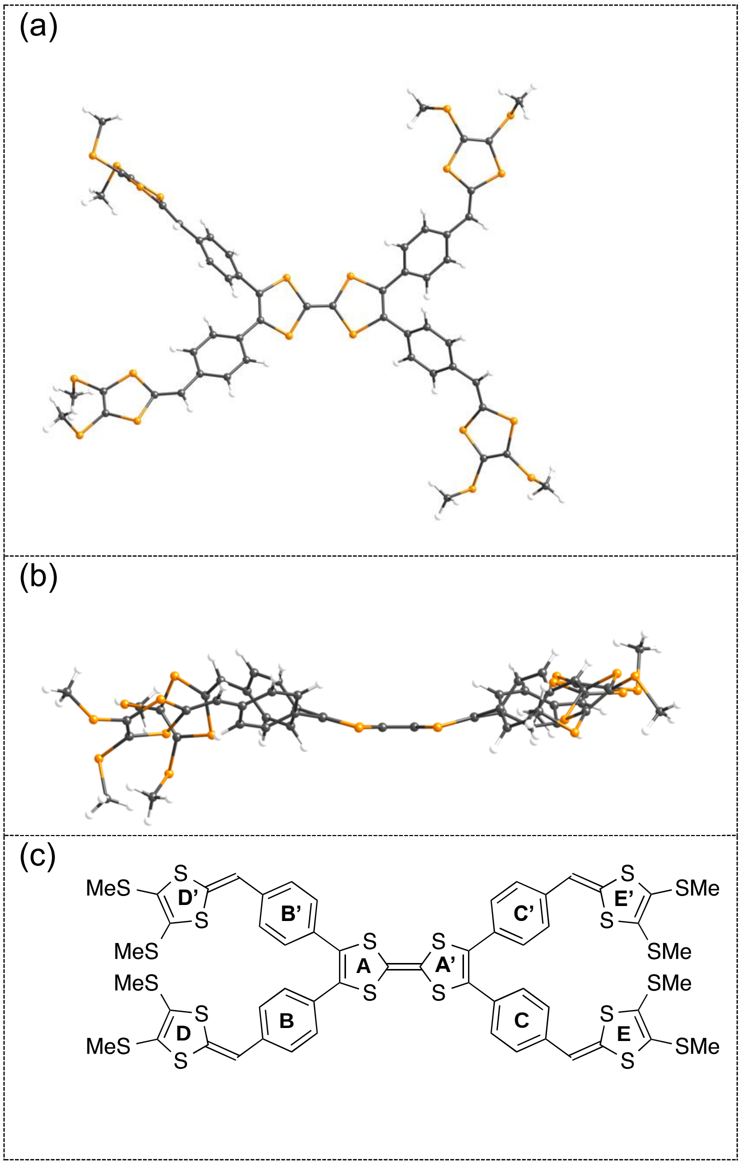

Figure 1: An optimized structure of **1a**; (a) top view, (b) side view, and (c) labeling of the 1,3-dithiole rings.

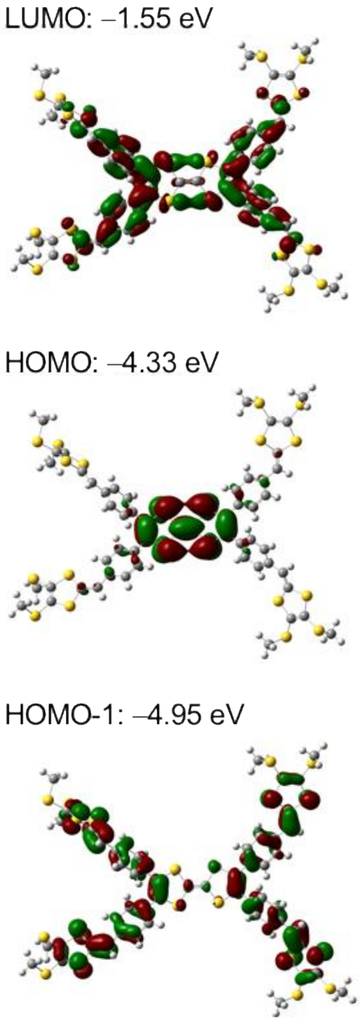

Figure 2: Molecular orbitals of **1a**.

The redox behaviors of **1–4** were investigated by cyclic voltammetry. Compounds **1a** and **1b** exhibited four and three pairs of redox waves, respectively (around +0.03 V, +0.10, +0.17, and +0.42 V vs. Fc/Fc^+ for **1a**; –0.05, +0.10, and +0.46 V vs. Fc/Fc^+ for **1b**) (Figure 3). The redox potentials of **1a,b** are summarized in Table 2 together with the related compound TTF. The redox waves observed at +0.42 V for **1a** and +0.46 V for **1b** are almost derived from the second redox of the TTF moiety, because they are close to the E_2 of TTF (+0.37 V). The remaining redox processes observed at around +0.03, +0.10, and +0.17 V for **1a**, and –0.05 and +0.10 V for **1b** might be derived from the first redox of the TTF moiety and the redox of the four outer 1,3-dithiole rings. To extract the exact oxidation potentials and number of electrons involved in each oxidation step, a digital simulation technique was applied [44]. As the result, the observed redox waves of **1a** were well reproduced by the simulated waves (Table 2). It was indicated that the redox wave at +0.10 V was observed as overlap of sequential two stages of one- and two-electron transfer waves at +0.07 and +0.12 V, while the other waves correspond to one-electron transfer processes. The simulation results of **1a** also showed that the redox wave simulated at +0.02 V might be derived from the TTF moiety because of the close ΔE values of them (ΔE = +0.40 V for **1a**; +0.46 V for TTF). The same discussion could be applicable for **1b**. In addition, the potentials in which the outer 1,3-dithiole rings of **1a,b** participate are influenced by their substituents, that is, **1b** bearing electron-donating methyl groups has more negative redox potentials than **1a**. As a consequence, the one-electron redox process of the TTF moiety and multi-electron redox processes of the outer 1,3-dithiole rings might overlap in **1b**. Compound **4** exhibited three pairs of redox waves (around –0.09, +0.09, and +0.53 V vs. Fc/Fc^+). The redox potentials of **4** and the simulation results are also summarized in Table 2 together with their related compounds TTF and **14**. The redox process observed at +0.53 V is almost derived from the second redox of the TTF moiety, because it is the closest in the value to the E_2 of TTF (+0.37 V) out of all of the potentials of the related compounds, TTF and **14**. The remaining redox processes observed at around –0.09 and +0.09 V might be derived from the first redox of the TTF moiety, and the overall redox of **14**-like sites, respectively. The observed potentials of **4** were generally consistent with the simulated ones. The results of a digital simulation also showed that the redox wave observed at around –0.09 V and +0.09 V correspond to three stages of one-electron transfer and six stages of one-electron transfer processes, respectively. In addition to overlap of the first redox of TTF and the redox of **14**-like sites, each redox potential of the succeeding eight-electron oxidations of four **14**-like sites might slightly shift due to the non-equivalence of four **14**-like sites. Also, the small *ΔE* value (*ΔE* = 0.16 V) of **14** makes the redox wave overlap. For these reasons, the first and second redox waves of **4** are broad, compared to those of **1a** and **1b**. The redox waves of **1a,b** and **4** derived from the second redox of the TTF moiety (+0.42 V for **1a**; +0.46 V for **1b**; +0.53 V for **4**) shifted to higher potentials than the second redox of TTF because of the instability of the hexacationic state of **1a,b** and decacationic state of **4** compared to the dicationic states of TTF caused by on-site Coulomb repulsion between positive charges in the central TTF moiety and the outer 1,3-dithiole rings. In addition, the observed peak currents of **1a** and **4** in high potential region at +0.4 − +0.5 V were smaller than those of the simulated waves. This phenomenon might be understood by considering that electron transfer of this redox reaction is slow enough to become a rate-determining step because of the crowded structure which the TTF core participating in this redox process is surrounded by extended aromatic rings bearing 1,3-dithiol rings. More details of the redox mechanisms of **1–4** are under investigation.

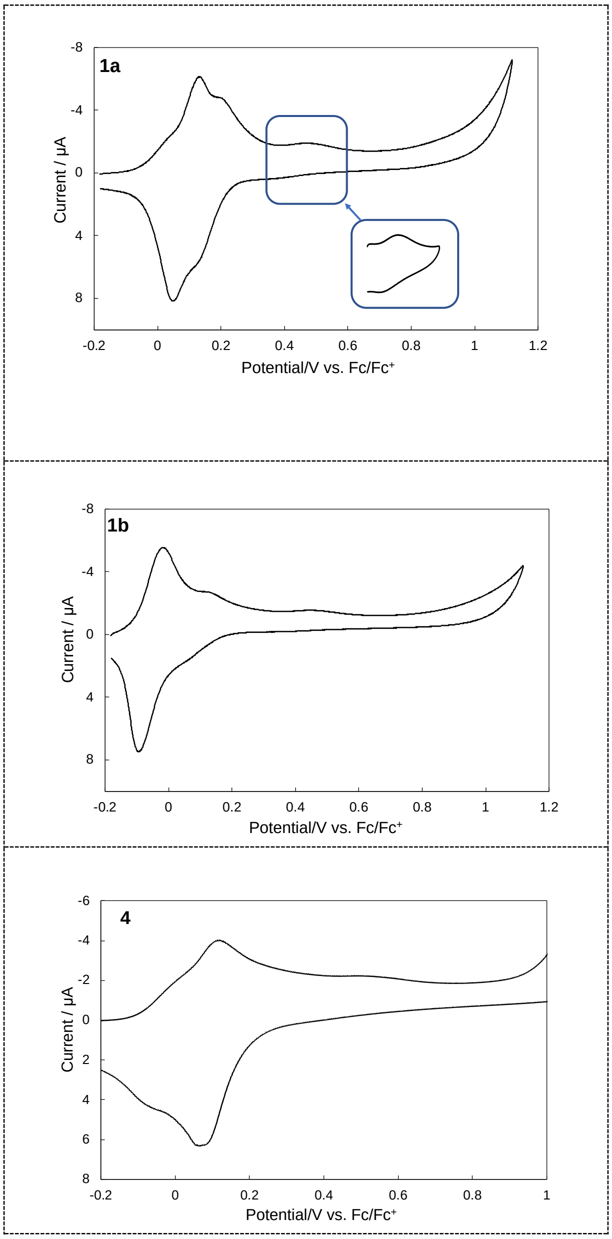

Figure 3: Cyclic voltammograms of **1a,b** and **4** in PhCN/CS_2 (1/1, V/V) solution.

Table 2: Redox potentials of **1**, **4**, and related compounds[a].

Compound	observed or simulated value	E_1	E_2	E_3	E_4	E_5	E_6	E_7	E_8	E_9	E_{10}
1a	observed	around +0.03[b]	+0.10			+0.17	+0.42				
	simulated	+0.02	+0.07	+0.12		+0.20	+0.42				
1b	observed	−0.05				+0.10	+0.46[b]				
4	observed	around −0.09			+0.09						+0.53[b]
	simulated	−0.06	−0.03	+0.01	+0.047	+0.053	+0.098	+0.102	+0.11	+0.18	+0.50
TTF[c]	observed	−0.09	+0.37								
14[c]	observed	−0.07	+0.09								

[a]In PhCN/CS_2 (1/1, V/V) containing 0.1 M $^{n}Bu_4NPF_6$. [b]Anodic peak. [c]In PhCN containing 0.1 M $^{n}Bu_4NPF_6$. All potentials measured against Ag/Ag$^+$ reference electrode and converted to vs. Fc/Fc$^+$.

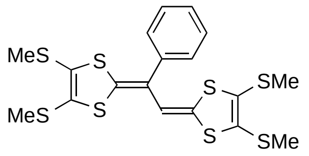

14

Chart 2: Related compound **14**.

Supporting Information

Supporting Information File 1:

File Name: DT-Aryl-TTF_SI

File Format: PDF

Acknowledgements

This work was partially supported by a Grant-in-Aid for Scientific Research (JP15H03798), from the Ministry of Education, Culture, Sports, Science and Technology (MEXT), Grants-in-Aid for Research Promotion to The Research Unit for Development of Organic Superconductors and The Research Unit for Power Generation and Storage Materials from Ehime University.

References

1. *TTF Chemistry-Fundamental and Applications of Tetrathiafulvalene*, ed. by Yamada, J.; Sugimoto, T.; Kodansha-Springer, Tokyo, 2004.

2. Canevet, D.; Sallé, M.; Zhang, G.; Zhang, D.; Zhu, D. *Chem. Commun.* **2009**, 2245–2269.

3. Gorgues A.; Hudhomme, P.; Sallé, M. *Chem. Rev.* **2004**, *104*, 5151–5184.

4. Segura, J. L.; Martín, N. *Angew. Chem. Int. Ed.* **2001**, *40*, 1372–1409.

5. Iyoda, M.; Hasegawa, M.; Miyake, Y. *Chem. Rev.* **2004,** *104*, 5085–5114.

6. Hasegawa, M; Iyoda, M. In *Organic Redox Systems*; Nishinaga, T. Ed.; Wiley: New Jersey, 2016; Chapter 4, pp 89–130.

7. Misaki, Y. *Sci. Technol. Adv. Mater.* **2009**, *10*, 024301. 1–22.

8. Inatomi, N.; Hojo, N.; Yamamoto, T.; Shimada, M.; Watanabe, S. *213th ECS meeting, Phoenix* **2008** Abstract #167.

9. Inatomi, Y.; Hojo, N.; Yamamoto, T.; Watanabe, S.; Misaki, Y. *ChemPlusChem,* **2012**, *77*, 973–976.

10. Kato, M.; Ogi, D.; Yao, M.; Misaki, Y. *Chem. Lett.* **2013**, *42*, 1556–1558.

11. Kato, M.; Senoo, K.; Yao, M.; Misaki, Y. *J. Mater. Chem. A* **2014**, *2*, 6747–6754.

12. Iwamoto, S.; Inatomi, Y. Ogi, D.; Shibayama, S.; Murakami, Y.; Kato, M.; Takahashi, K.; Tanaka, K.; Hojo, N.; Misaki, Y. *Beilstein J. Org. Chem.* **2015**, *11*, 1136–1147.

13. Yamauchi, T.; Shibata, Y.; Aki, T.; Yoshimura, A.; Yao, M.; Misaki, Y. *Chem. Lett*. **2018,** *47*, 1176–1179.

14. Ogi, D.; Fujita, Y.; Kato, M.; Yamauchi, T.; Shirahata, T.; Yao, M.; Misaki, Y. *Eur. J. Org. Chem.* **2019**, 2725–2728.

15. Yamauchi, T.; Kato, M.; Shirahata, T.; Yao, M.; Misaki, Y. *Chem. Lett*. **2019**, *48*, 1507–1510.

16. Bryce, M. R. *J. Mater. Chem.* **2000**, *10*, 589–598.

17. Coffen, D. L.; Chambers, J. Q.; Williams, D. R.; Garrett, P. E.; Canfield, N. D. *J. Am. Chem. Soc.* **1971**, *93*, 2258–2268.

18. Ueno, Y.; Okawara, M. *Chem. Lett.* **1974**, *3*, 1135–1138.

19. Ueno, Y.; Nakayama, A.; Okawara, M. *J. Am. Chem. Soc.* **1976**, *98*, 7740–7741.

20. Yoneda, S.; Kawase, T.; Inaba, M.; Yoshida, Z.-i. *J. Org. Chem.* **1978**, *43*, 595–598.

21. Coustumer, G. L.; Mollier, Y. *J. Chem. Soc., Chem. Commun.* **1980**, 38–39.

22. Babeau, A.; Tinh, N. H.; Gasparoux, H.; Polycarpe, C.; Torreilles, E.; Giral, L. *Mol. Cryst. Liq. Cryst.* **1982**, *72*, 171–176.

23. Starodub, V. A.; Baumer, V. N.; Guella, I. M.; Golovkina, I. F. *Synth. Met.* **1983**, *5*, 101–111.

24. Tsujimoto, K.; Okeda, Y.; Ohashi, M. *J. Chem. Soc., Chem. Commun.* **1985**, 1803–1804.

25. Charlton, A.; Underhill, A. E.; Williams, G.; Kalaji, M.; Murphy, P. J.; Hibbs, D. E.; Hursthouse, M. B.; Malik, K. M. A. *Chem. Commun.* **1996**, 2423–2424.

26. Charlton, A.; Underhill, A. E.; Williams, G.; Kalaji, M.; Murphy, P. J.; Malik, K. M. A.; Hursthouse, M. B. *J. Org. Chem.* **1997**, *62*, 3098–3102.

27. Hock, R. G. J. *Synth. Met.* **1997**, *84*, 339–340.

28. Zotti, G.; Zecchin, S.; Schiavon, G.; Berlin, A.; Huchet, L.; Roncali, J. *J. Electroanal. Chem.* **2001**, *504*, 64–70.

29. Kakinuma, T.; Kojima, H.; Kawamoto, T.; Mori, T. *J. Mater. Chem. C* **2013**, *1*, 2900–2905.

30. Mitamura, Y.; Yorimitsu, H.; Oshima, K.; Osuka, A. *Chem. Sci.* **2011**, *2*, 2017–2021.

31. Gholami, M. Tykwinski, R. R. *Chem. Rev.* **2006**, *106*, 4997–5027.

32. Sugimoto, T.; Awaji, H.; Misaki, Y.; Yoshida, Z.-i.; Kai, Y.; Nakagawa, H.; Kasai, N. *J. Am. Chem. Soc.* **1985**, *107*, 5792–5793.

33. Sugimoto, T.; Misaki, Y.; Arai, Y.; Yamamoto, Y.; Yoshida, Z.-i.; Kai, Y.; Kasai, N. *J. Am. Chem. Soc.* **1988**, *110*, 628–629.

34. Misaki, Y.; Matsumura, Y.; Sugimoto, T.; Yoshida, Z.-i. *Tetrahedron Lett.* **1989**, *30*, 5289–5292.

35. Amaresh, R. R.; Liu, D.; Konovalova, T.; Lakshmikantham, M. V.; Cava, M. P.; Kispert, L. D. *J. Org. Chem.* **2001**, *66*, 7757–7764.

36. Rajagopal, D. Lakshmikantham, M. V.; Cava, M. P. *Org. Lett.* **2002**, *4*, 2581–2583.

37. Coffin, M. A.; Bryce, M. R.; Batsanov, A. S.; Howard, J. K. *J. Chem. Soc., Chem. Commun.* **1993**, 552–554.

38. Bryce, M. R.; Coffin, M. A.; Skabara, P. J.; Moore, A. J.; Batsanov, A. S.; Howard, J. K. *Chem. –Eur. J.* **2000**, *6*, 1955–1962.

39. Hasegawa, M.; Fujioka, A.; Kubo, T.; Honda, T.; Miyamoto, H.; Misaki, Y. *Chem. Lett.* **2008**, *37*, 474–475.

40. Horiuchi, H.; Misaki, Y. *Chem. Lett.* **2010**, *39*, 989–991.

41. Nishiwaki, M.; Tezuka, M.; Shirahata, T.; Misaki, Y. *Chem. Lett.* **2011**, *40*, 467–469.

42. The molecular orbital calculation was carried out using the Gaussian 03 program: M. J. Frisch et al., *Gaussian 03*, Gaussian, Inc., Pittsburgh, PA, **2003**.

43. The optimized geometry and the LUMO, HOMO, and HOMO−1 levels of **3a** and **4** are shown in Figure S4.

44. The digital simulations were performed using DigiElch 7 Prof software.